

Investigation of the effect of a bar's inadequate embedded length on the P-M interaction curve of reinforced concrete columns with rectangular sections

Seyed Shaker HASHEMI*, Mohammad VAGHEFI

Civil Engineering Department, Persian Gulf University, Bushehr-IRAN

e-mail: sh.hashemi@pgu.ac.ir

Received: 11.03.2011

Abstract

In this research, the effects of embedded length and pull-out force on the seismic behavior of a reinforced concrete (RC) column were investigated. Separate degrees of freedom were used for the steel and concrete parts in the nonlinear modeling of the RC elements in order to consider the bond-slip effect. The analytical method was assessed through the comparison of experimental and analytical results. The effect of the bar's slippage on the axial force-bending moment (P-M) interaction curve of the RC column was calculated by nonlinear modeling of pull-out behavior. The P-M interaction curves for a variety of columns with different embedded bar lengths in the footing were calculated and compared. In most recommendations and instructions for the capacity of RC columns, it is assumed that the embedded length of the longitudinal bars in the joints is sufficient and slippage will not occur. However, in this research, the effect of reduction of the embedded length on the P-M interaction curve of RC columns was evaluated, and, in the end, a modification strategy was proposed for the curve suggested by the American Concrete Institute. The results show that as long as the embedded length is sufficient, responses do not differ significantly. By reducing the embedded length, much of the effect of the bar's pull-out on the P-M interaction curve occurs in terms of pure bending or low axial forces. By increasing the percentage of longitudinal bars, the capacity reduction increases due to the pull-out effect.

Key Words: Bar's pull-out, Embedded length, P-M interaction curve, Reinforced concrete column, Seismic analysis

1. Introduction

The analytical axial force-bending moment (P-M) interaction curve is a common curve in the design process of reinforced concrete (RC) columns. Using analytical relations and some assumptions, this curve can be simply calculated and extracted. According to American Concrete Institute (ACI) document ACI 318-08 (2008), these curves are calculated depending on the following assumptions:

*Corresponding author

- the strain distribution in the RC cross-section is linear,
- shear deformation is not considered, and
- a perfect bond is assumed between the bars and the surrounding concrete.

Currently, P-M curves are calculated based on the existence of compatibility between the concrete and bar deformations in the RC section (Figure 1). In other words, the bond between the concrete and the bars is assumed to be perfect, and slip is neglected. However, the bond between the concrete and the bars is not complete, and this may affect the accuracy of the calculations.

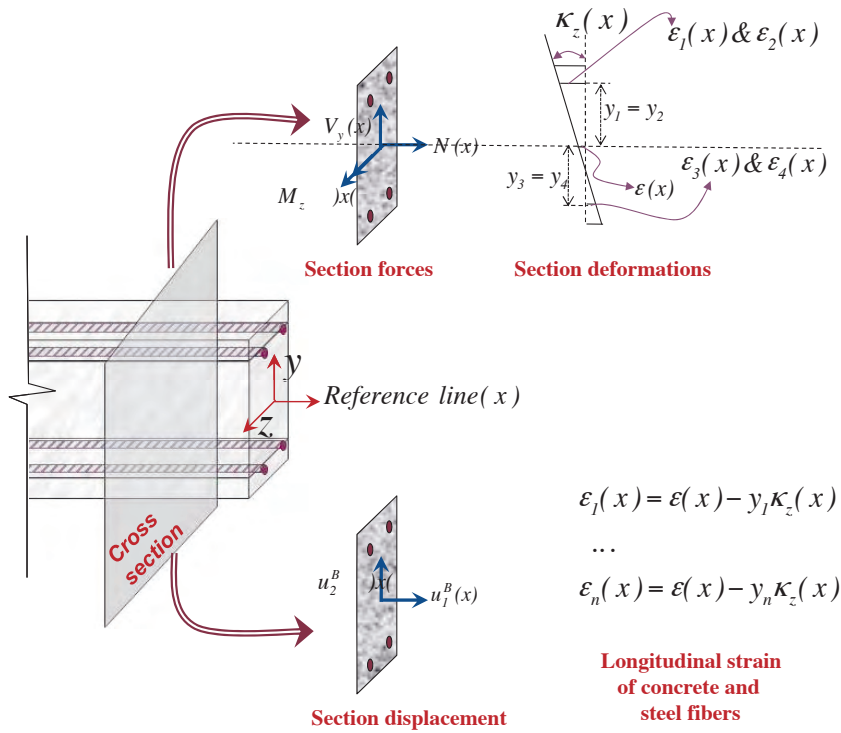


Figure 1. Cross-sectional details of a RC section.

The footing position of the RC column is considered to be one of the critical zones of RC structures. Therefore, to check and control the seismic behavior and design of many columns, the critical control section is the column footing section. The embedded length of the longitudinal bars in the footing connection is one of the influential parameters in determining the capacity of RC columns. Currently, based on ACI 318-08 regulation criteria, the embedded length of longitudinal bars is assumed to be sufficient and the pull-out effect is ignored. On the other hand, in the design process, special arrangements are recommended to provide enough embedded length to prevent the pull-out of the bars. If, however, due to reasons such as executive problems or faults, a sufficient embedded bar length is not provided, then the ACI 318-08 regulation for P-M interaction curves cannot be used to evaluate or estimate the RC column capacity. Such a condition is applicable in the case of the seismic vulnerability of RC columns previously made with inadequate embedded lengths of longitudinal bars. In this research, we examined the ways by which the curve for conditions affected by reduced embedded length can be changed. For this purpose, in a nonlinear analysis process with consideration of the bond-slip effect and

the bar's strain, necessary analysis was done for several samples with different percentages of longitudinal bars. In addition, the results were compared with the ACI 318-08 recommended values.

In the present study, for a short concrete column not affected by the effects of slenderness, the effect of the bar's pull-out from the footing on the P-M interaction curve was investigated. The layer model was used for numerical modeling. In this method, an element is divided into a number of concrete and steel fiber lengths, and the element section specifications are worked out by adding up the effects of the fibers' behavior. The layer method assumes a perfect bond between the concrete and the bar (Spacone et al., 2002), but this assumption is neither appropriate nor realistic, and it causes a considerable difference between the analytical and experimental results (Kwak and Kim, 2006). Limkatanyu and Spacone (2002) used the layer model, but they removed the perfect bond assumption. In order to achieve this goal, they separated the degrees of freedom of the concrete from the bars in the beam-column elements. However, for modeling RC frames, a joint element is also needed. What matters is the compatibility and assimilability of joint elements with beam-column elements. In this study, the beam-column element introduced by Limkatanyu and Spacone (2002) was used to model the column element because it has good precision and includes the interaction between the concrete and the bars. A joint element that is capable of being assembled with the above column element was also defined and used. Moreover, this modeling takes into consideration the pull-out effect of the bars that are restrained within joints.

2. Nonlinear modeling of the RC columns with the joint element

For the purpose of nonlinear analysis of RC columns and investigation of the bond-slip effect, 2 types of columns and joint elements were modeled (Figure 2). A computer program created in MATLAB software was used (MathWorks, 2008). For modeling a column element based on the research carried out by Limkatanyu and Spacone (2002), in the fiber model, the slip effect between the concrete and the bar was implemented without ignoring the compatibility of the strain between them. In this method, a length segment of a RC frame element is considered as the combination of a length segment of a 2-node concrete element and a number of steel bar elements. The 2-node concrete elements follow the Euler-Bernoulli beam theory, and the 2-node bar elements are, in fact, truss elements. The contact between the concrete and the longitudinal bars is provided by a constant bond force around the bars. The governing equations of the length segment of the RC element are obtained by using the internal force balance equations as well as the concrete element axial force equations, steel bar element equations, shear force balance, and flexural force balance in the length segment. A weak form of the governing equation in a finite element method was obtained using the shape functions based on displacement and using the principle of stationary potential energy.

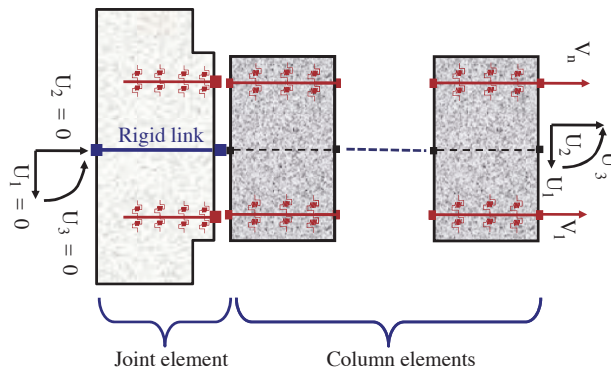


Figure 2. Numerical modeling of a RC column with footing connection.

A joint element was used as the footing connection of the RC column. In this element, the effect of pull-out is considered as the relative displacement between the steel bar and the surrounding concrete, and bond stress is referred to as the shear stress acting parallel to an embedded steel bar on the contact surface between the reinforcing bar and the concrete (Figure 3). Referring to Figure 3, the slippage of the bars can be defined in the form of Eq. (1), if the nodal displacement vector related to pull-out behavior is defined as $\mathbf{U}_{PM} = [U_1 \ U_2 \ U_3 \ V_1 \ \dots \ V_n]^T$.

$$\mathbf{PO} = \begin{bmatrix} s_1 \\ s_2 \\ \vdots \\ s_n \end{bmatrix} = \begin{bmatrix} -1 & 0 & y_1 & 1 & 0 & \dots & 0 \\ -1 & 0 & y_2 & 0 & 1 & \dots & 0 \\ \vdots & \vdots & \vdots & \vdots & \vdots & \vdots & \vdots \\ -1 & 0 & y_n & 0 & 0 & \dots & 1 \end{bmatrix} \mathbf{U}_{PM} = \mathbf{A}_{PM} \mathbf{U}_{PM} \quad (1)$$

In this equation, y_n is the distance of the n th bar from the reference line. The relationship between pull-out force and slip for the embedded n th bar in the section can be defined as $f_{PO\ n} = k_{PO\ n} \times d_{b_n}$, where $f_{PO\ n}$ is the pull-out force and $k_{PO\ n}$ is the slip stiffness of the pull-out behavior. This equation derives from the bond stress-slip relationship related to the pull-out behavior, the embedded length of the bar, and the conditions at the end of the bar and the perimeter of the bar cross-section. The relationship between the pull-out force and the slip of all bars in the section can be written in the matrix form below.

$$\mathbf{f}_{PO} = \mathbf{k}_{PO} \times \mathbf{PO}$$

$$\begin{bmatrix} f_{PO\ 1} \\ f_{PO\ 1} \\ \dots \\ f_{PO\ n} \end{bmatrix} = \begin{bmatrix} k_{PO\ 1} & 0 & \dots & 0 \\ 0 & k_{PO\ 2} & \dots & 0 \\ \dots & \dots & \dots & \dots \\ 0 & 0 & \dots & k_{PO\ n} \end{bmatrix} \times \begin{bmatrix} d_{b_1} \\ d_{b_2} \\ \dots \\ d_{b_n} \end{bmatrix}_{n \times 1} \quad (2)$$

The nodal force vector can be expressed in the following form:

$$\mathbf{F}_{PM} = \mathbf{A}_{PM}^T \times \mathbf{f}_{PO} = \mathbf{A}_{PM}^T \times \mathbf{k}_{PO} \times \mathbf{PO} = \mathbf{A}_{PM}^T \times \mathbf{k}_{PO} \times \mathbf{A}_{PM} \times \mathbf{U}_{PM} = \mathbf{K}_{PM} \times \mathbf{U}_{PM}. \quad (3)$$

From Eq. (3), the pull-out stiffness matrix can be written as $\mathbf{A}_{PM}^T \times \mathbf{k}_{PO} \times \mathbf{A}_{PM}$. The pull-out stiffness matrix will be imposed onto the stiffness matrix of the joint element. In order to calculate the resisting force vector related to pull-out behavior and to impose it onto the resisting force vector of the joint element, it can be written in the form of $\mathbf{A}_{PM}^T \times \mathbf{f}_{PO}$.

2.1. Concrete and steel materials' stress-strain relationships

The monotonic envelope curve for confined concrete, introduced by Park et al. (1972) and later extended by Scott et al. (1982), was adopted for the compression region because of its simplicity and computational efficiency (Figure 4a). It was assumed that the concrete behavior is linearly elastic in the tension region before the tensile strength and that, beyond that, the tensile stress decreases linearly with increasing tensile strain (Figure 4b). In tensile behavior, ultimate failure from cracking is assumed to occur when the tensile strain exceeds the value given in Eq. (4).

$$\varepsilon_{ut} = 2 \times (G_f/f_t) \times \ln(3/L)/(3-L) \quad (4)$$

Here, L denotes the element length in millimeters and G_f is the fracture energy, dissipated in the formation of a crack of unit length per unit thickness and considered as a material property. f_t is the concrete tensile strength. For normal-strength concrete, the value of G_f/f_t is in the range of 0.005-0.01 (Welch and Haisman, 1969). In this research, the value of G_f/f_t was assumed to be an average value of 0.0075.

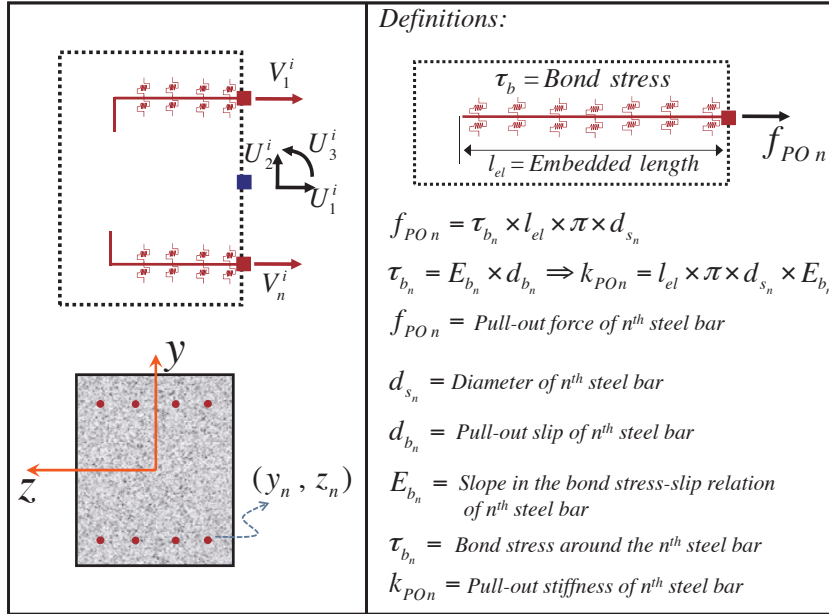


Figure 3. Numerical modeling of the bar's pull-out.

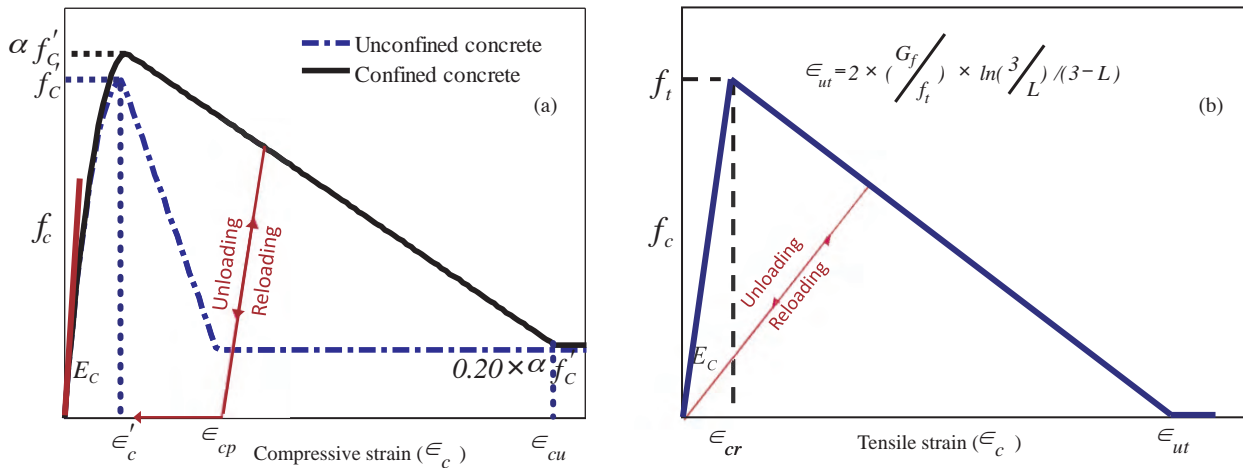


Figure 4. Concrete stress-strain relationship: a) compressive behavior, b) tensile behavior.

The Giuffre-Menegoto-Pinto model was adopted to represent the stress-strain relationship of the steel bars (Figure 5). This model was initially proposed by Giuffre and Pinto (1970) and later used by Menegoto and Pinto (1973).

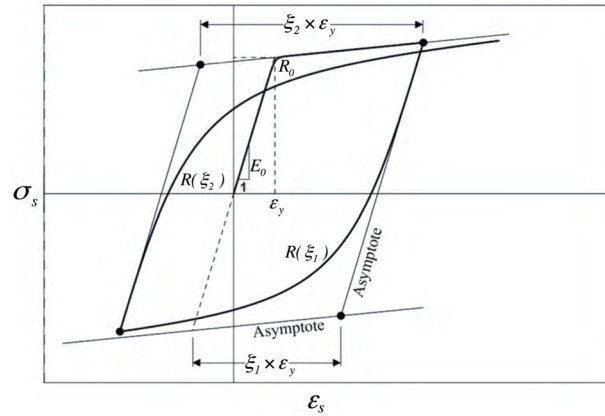


Figure 5. Stress-strain relationship of the bars.

2.2. Bar and concrete interaction

Bond stress is referred to as the shear stress acting parallel to an embedded steel bar on the contact surface between the reinforcing bar and the concrete. Bond slip is defined as the relative displacement between the steel bar and the concrete. In this paper, 2 models were used for the bond stress-bond slip relationship, 1 for the bond-slip behavior through the length of the beam-column elements, and 1 for the pull-out behavior of the bars in the joint elements. Among the several models proposed by researchers, that proposed by Eligehausen et al. (1983) was adopted (Figure 6). In this model, the effect of many variables, such as the spacing and height of the lugs on the steel bar, the compressive strength of the concrete, the thickness of the concrete cover, the steel bar diameter, and the end bar hooks, are considered. Moreover, this model was investigated and proposed as a good and accurate model (Gan, 2000).

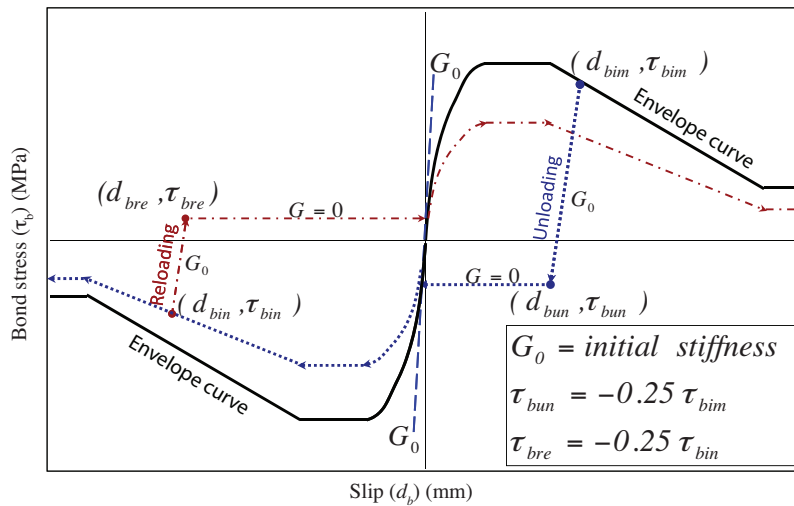


Figure 6. Bond stress-slip relationship (Gan, 2000).

3. Numerical investigation

For numerical investigation, first, for a RC column with the geometric specifications given in Figure 7 and the characteristics given for specimen 2 in Table 1, numerical validation was done. This specimen is a column under

uniaxial bending and a constant axial load with a magnitude of 350 kN. Lateral cyclic displacement was imposed at the free end. It was tested by Qiu et al., who gave more details (2002). In numerical modeling, the column is subdivided into a sufficient number of shorter elements. Because the formulation is displacement-based and the response depends on the element size, it is necessary that the length of the elements be short enough. As a simple suggestion, the length of the column elements can be selected as equal to or smaller than the average crack spacing in the beam or in the column. In these cases, convergence of the calculated responses will be achieved in the numerical process. For nonlinear solving of this model, a Newton-Raphson method, which included the controlling of displacement, was used. According to Figure 8, verification shows that the analytical and experimental load-displacement history was in good accordance with the strength, stiffness, and changes during cyclic loading.

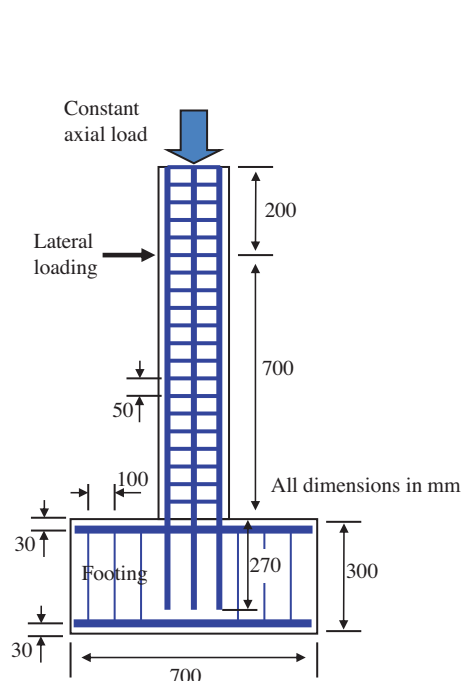


Figure 7. Geometry of the specimens (Qiu et al., 2002).

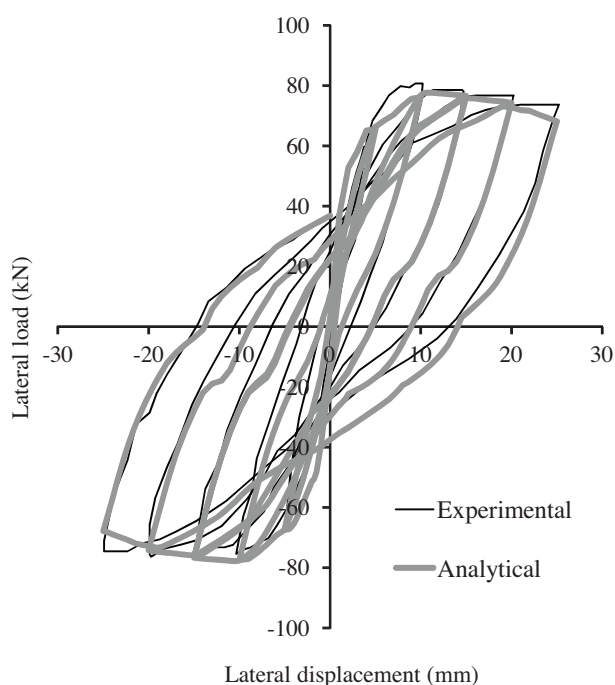
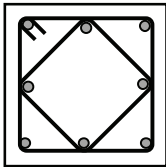
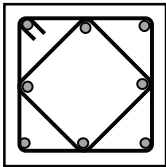
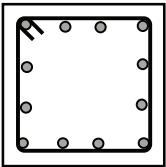


Figure 8. Experimental and analytical cyclic load-displacement responses for specimen 2.

After ensuring the accuracy and precision of the analytical method, a P-M curve was calculated in relation to a cross-section with zero distance from the footing connection of a column with geometric specifications according to Figure 7. The calculation was repeated for a variety of embedded lengths and percentages of longitudinal bars. Three specimens (specimens 1, 2, and 3), which respectively had 1.57%, 2.26%, and 3.39% longitudinal bars, were analyzed. More details about these specimens are given in Table 1. The analytical results for specimen 1 relevant to various embedded lengths are presented in Figure 9. Likewise, the results for specimens 2 and 3 are given in Figures 10 and 11, respectively. According to the ACI 318-08 requirements, the required embedded length of the longitudinal bars in the footing is given in Table 2. The minimum required embedded length is sufficiently conservative considering the computational embedded length based on ACI 318 formulas, and results show that as long as the embedded length is sufficient (equal to or greater than the ACI 318 suggested value), responses do not differ significantly. However, with considerable reduction of the embedded

Table 1. Details of investigated specimens.

	Specimen 1 $\rho = 1.57\%$	Specimen 2 $\rho = 2.26\%$	Specimen 3 $\rho = 3.39\%$
Section view			
Main bars	8 × 10 mm bars	8 × 12 mm bars	12 × 12 mm bars
Stirrups	6 mm bars @ 50 mm c/c	6 mm bars @ 50 mm c/c	6 mm bars @ 50 mm c/c
Cross section (width × depth)	200 × 200 mm ²	200 × 200 mm ²	200 × 200 mm ²
f_c (MPa)	40	40	40
f_y of main bars (MPa)	460	460	460
f_y of stirrups (MPa)	420	420	420
Concrete cover (mm)	21	21	21

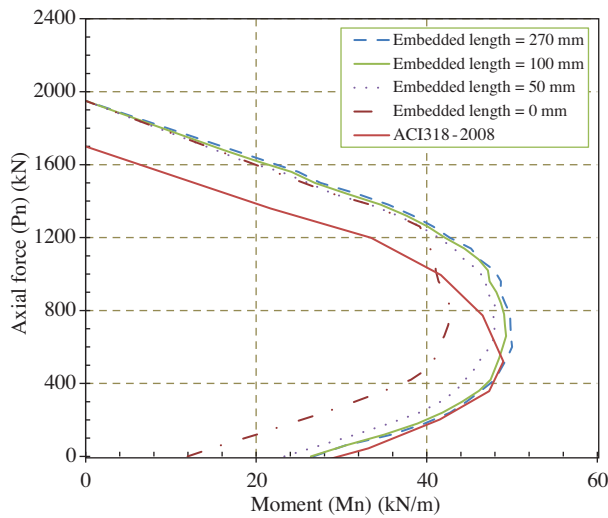


Figure 9. P-M interaction curve calculated for specimen 1.

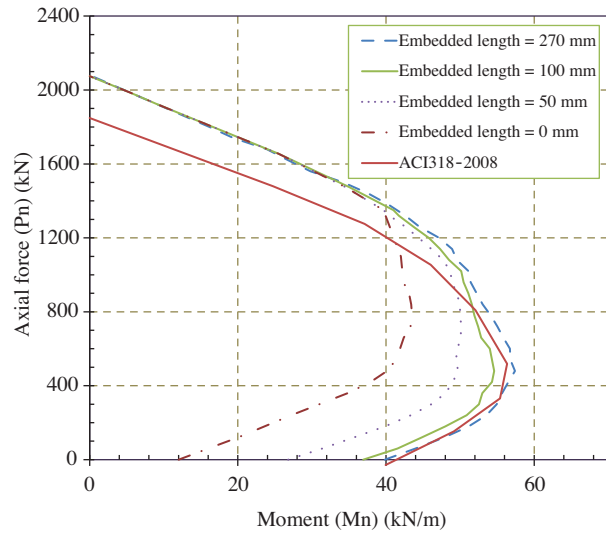


Figure 10. P-M interaction curve calculated for specimen 2.

length, the P-M curves will change and the bending capacity of the RC column will decrease. By evaluating responses from all 3 specimens, we can say that the greatest effect of the bar's pull-out on the P-M interaction curve occurs in terms of pure bending or low axial forces. According to Figure 12, the P-M curve can be divided into 3 parts. The part in which the bending behavior is predominant receives the highest effect. In the part in which the axial force in the section of the column is considerable, the reduction of the embedded length does not significantly affect the capacity of the column. This is because, in the presence of a large axial force, the longitudinal bars of the section are always under compression and the tensile force that leads to pull-out does not occur. When the values of both axial force and bending moment are considerable, depending on the tensile stress created in the bars, the pull-out will affect the column capacity. The results also show that by increasing

the percentage of longitudinal bars and emphasizing the role of the steel bars more than that of the concrete, the decreased amount of capacity due to pull-out effect is greater. Where the embedded length is equal to zero, the ultimate bending capacity is calculated based on the concrete tensile strength for a fully cracked section. The bending capacity is thus calculated as a section without longitudinal bars for all 3 specimens, and in pure bending conditions, the ultimate bending capacities are equal. Meanwhile, an embedded length of zero means that the longitudinal bars of the column have not been continued into the foundation.

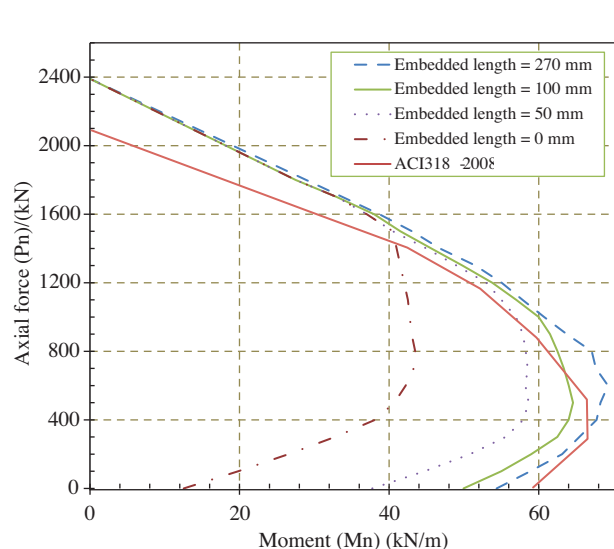


Figure 11. P-M interaction curve calculated for specimen 3.

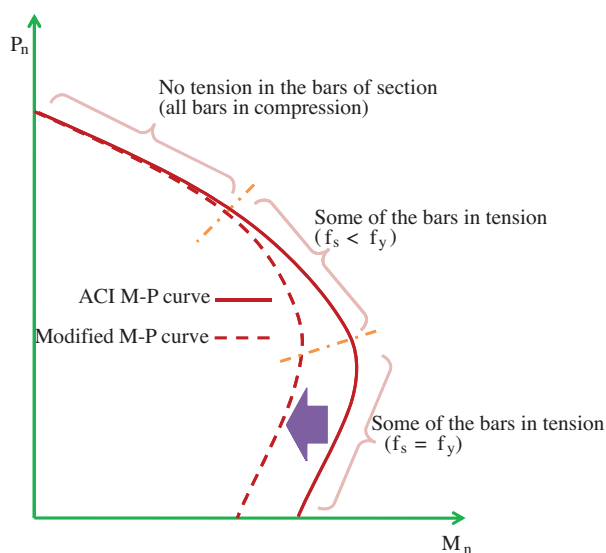


Figure 12. Schematic P-M interaction curve with the reducing effect of pull-out effect.

Table 2. Required embedded length of the specimens according to ACI 318.

		Specimen 1	Specimens 2 and 3
Without standard hook in the end of bar	Calculated required embedded length based on ACI 318 formulas (mm)	66	79
	Minimum required embedded length based on ACI 318 (mm)	300	300
With standard hook in the end of bar	Calculated required embedded length based on ACI 318 formulas (mm)	58	69
	Minimum required embedded length based on ACI 318 (mm)	150	150

In addition, the analytical results were compared with the ACI 318-08 recommendations. It should be remembered that ACI 318-08 stated that the P-M interaction curves depend on assumptions such as the embedded length being long enough and the bond between the bars and the surrounding concrete being perfect. In comparison with the analytical results when the embedded length is sufficient, good accordance can be seen in the pure bending mode. In the presence of axial force and especially with an increase in its value, however, the amount of difference will be significant. Reviewing the ACI 318-08 assertions, the major cause of dispute is that the increasing effect of confinement stirrups on the concrete's compressive strength was not considered in the ACI 318-08 formulas. In numerical analysis, however, the confinement effect is considered. In the pure bending mode or in the presence of a very low axial force, the criterion for reaching ultimate bending capacity is the bar's yielding without a significant role for the concrete's compressive strength, so the role of the concrete's ultimate

compressive strength in the ultimate capacity of the RC section is small and the yielding of the bars is more effective. Another cause for divergence between the analytical results and the ACI recommendations is that the numerical method employed is an analytical approach based on fiber theory and including the bond-slip effect, whereas the ACI recommendation used the assumption of compression block in the section. Naturally, these 2 methods are not identical. When the embedded length is sufficiently long, the ACI 318-08 P-M interaction curve does not need modification for the sake of pull-out and the bond-slip effect; moreover, it is assured and conservative. In reducing the embedded length, however, it is necessary to modify the P-M curve based on the ACI 318-08 recommendations. The proposed modification is that if $A_s f_s$ is smaller than f_{PO} , reforms are not done to the curve, but if this ratio is not established, f_{PO} should be used instead of $A_s f_s$ in the process of capacity calculation. Here, A_s and f_s are the area of the cross-section and the tensile stress of each bar, respectively. The f_{PO} value can be calculated according to the details given in Figure 3. In order to calculate τ_b , the relationship proposed by Eligehausen et al. (1983) can be used as in Eq. (5). In this equation, d_s is the bar's diameter in millimeters, f'_c is the concrete compressive strength in MPa, and τ_b will be calculated in MPa.

$$\tau_b = \left(20 - \frac{d_s}{4}\right) \left(\frac{f'_c}{30}\right)^{0.5} \tag{5}$$

The proposed modified method was validated for all specimens with good precision; as an example, the results for specimen 2 for an embedded length of 50 mm are presented in Figure 13.

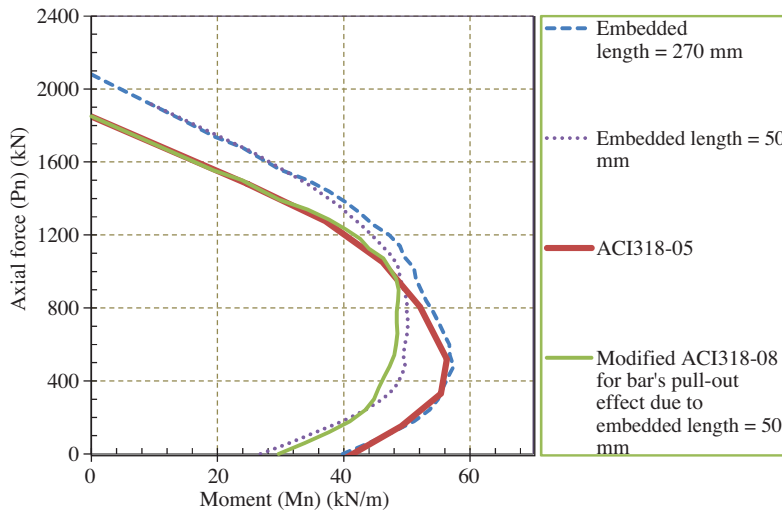


Figure 13. Inserting the reducing effect of the bar's pull-out into the P-M interaction for specimen 2.

4. Conclusion

As long as the embedded length is sufficient, responses do not differ significantly. By reducing the embedded length, the greatest effect of the bar's pull-out on the P-M interaction curve occurs in terms of pure bending or low axial forces. The results also showed that by increasing the percentage of longitudinal bars and highlighting the role of steel bars more than that of concrete, due to the pull-out effect, the amount of capacity reduction increases. In addition, comparison of the analytical results with ACI 318-08 recommendations showed that when the embedded length is sufficiently long, the ACI 318-08 P-M interaction curve does not need modification for the sake of pull-out and bond-slip effect; it is also assured and conservative. When the embedded length is reduced,

however, it is necessary to modify the P-M curve based on ACI 318-08. The modified method proposed here can be used for the modification process with good precision.

Acknowledgment

This research was supported by a grant from the Office of the Vice President for Research, Persian Gulf University. The authors hereby thank them for their financial aid.

References

- American Concrete Institute, Building Code Requirements for Structural Concrete and Commentary - ACI 318R, American Concrete Institute, Farmington Hills, Michigan, 2008.
- Eligehausen, R., Popov, E. and Bertero, V., Local Bond Stress-Slip Relationship of Deformed Bars under Generalized Excitations, Report No. UCB/EERC-83/23, Earthquake Engineering Center, University of California, Berkeley, 1983.
- Gan, Y., Bond Stress and Slip Modeling in Nonlinear Finite Element Analysis of Reinforced Concrete Structures, MSc Thesis, Department of Civil Engineering, University of Toronto, 2000.
- Giuffre, A. and Pinto, P.E., "Il Comportamento del Cemento Armato per Sollecitazioni Cicliche di forte Intensita", *Giornale del Genio Civile*, 108, 391-408, 1970.
- Kwak, H.G. and Kim, J.K., "Implementation of Bond-Slip Effect in Analyses of RC Frames under Cyclic Loads Using Layered Section Method", *Engineering Structures*, 28, 1715-1727, 2006.
- Limkatanyu, S. and Spacone, E., "Reinforced Concrete Frame Element with Bond Interfaces. Part I: Displacement-Based, Force-Based, and Mixed Formulations", *Journal of Structural Engineering*, 128, 346-355, 2002.
- MathWorks, MATLAB - The Language of Technical Computing, Version 7.6.0, MathWorks, Natick, Massachusetts, 2008.
- Menegoto, M. and Pinto, P., "Method of Analysis for Cyclically Loaded RC Plane Frames Including Changes in Geometry and Non-Elastic Behavior of Elements under Combined Normal Force and Bending", *Symposium on Resistance and Ultimate Deformability of Structures Acted on by Well-Defined Repeated Loads*, IABSE Reports, Vol. 13, Lisbon, 1973.
- Park, R., Kent, D.C. and Sampson, R.A., "Reinforced Concrete Members with Cyclic Loading", *Journal of the Structural Division*, 98, 1341-1360, 1972.
- Qiu, F., Li, W., Pan, P. and Qian, J., "Experimental Tests on Reinforced Concrete Columns under Biaxial Quasi-Static Loading", *Engineering Structures*, 24, 419-428, 2002.
- Scott, B.D., Park, R. and Priestley, M.J.N. "Stress-Strain Behavior of Concrete Confined by Overlapping Hoops at Low and High Strain Rates", *ACI Journal*, 79, 13-27, 1982.
- Spacone, E., Filippou, F.C. and Taucer, F.F., "Fibre Beam-Column Model for Nonlinear Analysis of R/C Frames: Part I. Formulation", *Earthquake Engineering and Structural Dynamics*, 25, 711-725, 1996.
- Welch, G.B. and Haisman, B., *Fracture Toughness Measurements of Concrete*, Report No. R42, University of New South Wales, Sydney, 1969.